Journal of Engineering and Applied Sciences 13 (10): 3555-3561, 2018
ISSN: 1816-949X

Structural and Solar Cell Properties of CuO Doped TiO_2 Thin Films Prepared by Laser Induced Plasma

[1]Sabah N. Mazhir, [1]Hanaa M. Yaseen, [1]Mona M. Salih and [2]Ghuson H. Mohamed
[1]Department of Physics, College of Science for Woman,
[2]Department of Physics, Collage of Science, University of Baghdad, Baghdad, Iraq

Abstract: In this study, Pulsed Laser Deposition technique (PLD) was utilized in this study to prepare to pure and CuO doped TiO_2 thin films and different weight ratios of CuO namely of (x = 0.0, 0.05, 0.1, 0.15 and 0.2) wt.% were deposited twice, on a glass slide and another on n-type silicon wafer substrates. Laser Nd-YAG with λ = 1064 nm, energy = 800 mJ and number of shots = 500 has been used in this experiment. Crystal structure and surface morphology have been investigated by X-Ray Diffraction (XRD) and AFM spectroscopy. The results reveal that the prepared $(TiO_2)_{1-x}$, $(CuO)_x$ thin films are polycrystalline, tetragonal structure and preferred orientation along 2θ around were 25.30 along (011) plane. AFM measurements confirmed that the films have good crystalline and homogeneous surface. The Root Mean Square (RMS) values showed that surface roughness and grain size of the thin films increased when CuO contents increase. The efficiency and solar cell parameters estimated from the I-V curves under dark and illumination were measured and the highest values of J_{sc}, V_{oc}, FF and efficiency of the fabricated solar cell were 1.0 mA, 1.6 V, 0.534 and 2.138%, respectively for $(TiO_2)_{0.8}$, $(CuO)_{0.2}$. Therefore, TiO_2:CuO nanocomposite is a good selection and improves the solar cell efficiency.

Key words: TiO_2:CuO solar cell, structural properties, pulse laser deposition technique, improves, homogeneous, morphology

INTRODUCTION

The optical and electrical properties of Titanium dioxide has been studied intensively all over the world in many spots (Linsebigler *et al*., 1995; Oehrlein, 1986). Due to the high dielectric constant of TiO_2 films, they have been used in fabricating capacitors in microelectronics devices (Wilmsen, 1985; Messick, 1976). (TiO_2) thin films own high band energy gap for allowed and forbidden direct transition about (3.2-3.29) and (3.69-3.78) eV correspondingly (Mechiakh and Bensaha, 2006). Crystalline TiO_2 film exist in three phases: rutile (tetragonal with a = 0.4594, c = 0.2958 nm), anatase (tetragonal with a = 0.3785, c = 0.9514 nm) and brookite (orthorhombic with a = 0.9184, b = 0.5447, c = 0.5145 nm), rutile being the most stable of the three and the formation of its phase depends on the starting material, deposition method and temperature treatment. In other words by changing temperature, TiO_2 thin films may take different forms for example from amorphous phase into crystalline anatase and from anatase into rutile (Leprince-Wang and Yu-Zhang, 2001; Mazhir *et al*., 2015). Rutile is usually the dominant phase in TiO_2 films but in some recent work, anatase-rich films have been synthesized. To prepare TiO_2 film, different deposition techniques were utilizded namely: thermal or anodic (Kozlowski *et al*., 1989) oxidation of titanium, electron beam evaporation (Lottiaux *et al*., 1989), chemical vapor deposition (Yeung and Lam, 1983), plasma-enhanced chemical vapor deposition (Williams and Hess, 1983), sol-gel method (Yaseen *et al*., 2016; Gartner *et al*., 1993) and reactive sputtering techniques (Suhail *et al*., 1992; Meng *et al*., 1993). Lately, thin films have been prepared by laser in so-called techniques Pulsed Laser Deposition (PLD) Lately, thin films has been prepared by laser in so-called techniques Pulsed Laser Deposition (PLD): Laser-induced plasma can constitute from the interaction of high-power Nd:YAG laser with solid medium (Mazhir, 2018). Smith and Turner (1965) were the first two how applied the a for mention technique, thin films are prepared by the ablation of one or more targets illuminated by a focused pulsed-laser beam for the preparation of semiconductor and dielectric thin films and was established due to the work of on high-temperature superconductors (Dijkkamp *et al*., 1987). Copper oxides are semiconductors that have been studied for several reasons such as the natural abundance of starting material Copper (Cu) the easiness of production by Cu oxidation their non-toxic

Coprresponding Author: Sabah N. Mazhir, Department of Physics, College of Science for Woman, University of Baghdad, Baghdad, Iraq

nature and the reasonably good electrical and optical properties (Papadimitropoulos *et al*., 2006). Copper forms tenorite (CuO), p-type semiconductors having band gap energy of 1.21-1.51 eV (Yoon *et al*., 2000; Oral *et al*., 2004). As a p-type semiconductor, conduction arises from the presence of holes in the valence band due to doping/annealing. CuO is considered as a good selective solar absorber due to its low thermal emittance and high solar absorbance (Banerjee and Chattopadhyay, 2005). Thick and thin polycrystalline CuO films were prepared in previous research using various methods such as Plasma evaporation and reactive sputtering and molecular beam epitaxy (Ristoy *et al*., 1985; Mazhir and Harb, 2015).

MATERIALS AND METHODS

Experimental details

Sample preparation: Titanium dioxide from nano shell company with a purity 99.99% and copper oxide with purity 99.99% were mixed at different concentrations Copper oxide of (x = 0.0, 0.05, 0.1, 0.15, 0.2) wt.%. The powder of precursor was mixed together using agate mortar, the mixture was then pressed into pellets (1.5 cm) in diameter and (0.2 cm) thick using hydraulic posten type (SPECAC), under pressure of 5 tons. The pellets were sintered in air at temperature (773 K) for 3 h. Thin films preparation of $(TiO_2)_{1-x}$, $(CuO)_x$ by PLD: $(TiO_2)_{1-x}$, $(CuO)_x$ films were deposited on glass slides substrates of (10×10 mm) at room temperature and different concentration of CuO. The glass substrate was cleaned with distilled water. Finally, deposited thin films from TiO_2: CuO by PLD technique using Nd: YAG with (λ = 1064 nm) SHG Q-switching laser beam at 800 mJ, repetition frequency (6 Hz) with 500 pulses is incident on the target surface making an angle of 45° with it as shown in Fig. 1. The distance between the target and the substrate was (1.5 cm), under a vacuum of (10^{-3} mbar).

Characterization: XRD analysis using SHIMADZU 6000 X-ray diffractometer system was employed in order to obtain the crystal quality and phase structure of the films. The surface morphology of the prepared films have been studied by using atomic force microscopy CSP Model AA3000 AFM supply by Angstrom company. The film thickness (t) was 25 nm measured using the optical interferometer method and He-Ne Laser (632.8 nm) is used. I-V measurements were done for $(TiO_2)_{1-x}(CuO)_x$/p-Si heterojunctions when they were exposed to Halogen lamp light Philips (120 W) with 50 mW/cm^2 intensity using Keithley Digital Electrometer 616, voltmeter and DC power supply under reverse and forward bias voltage which were in the range (-1 to 2) volt.

Fig. 1: PLD set up using Nd: YAG

RESULTS AND DISCUSSION

XRD studies: The crystal structure of $(TiO_2)_{1-x}$, $(CuO)_x$ recognized by a study of the phase of XRD for that material. Figure 2a-c shows the XRD patterns obtained for $(TiO_2)_{1-x}$ $(CuO)_x$ thin films deposited on a glass substrate with thickness of 200 nm by pulsed laser deposition method at different concentration of CuO x = (0.0, 0.05, 0.1, 0.15, 0.2) wt.% prepare at RT. According to American Society for Testing Materials (ASTM) cards, the prepared films showed a polycrystalline tetragonal structure for TiO_2 of Anatase phase. From Fig. 2, it can be observed that the preferred orientation was along (011) plane. In the X-ray patterns, it is clear that the peaks intensities increase with increasing of the doping ratio from 5-20%. Also, it was noticed that the all film quality improves with the increasing of CuO content and appear a new peak at all CuO concentrations which recognized as CuO structure that corresponds to the reflection plane of (111).

The interplaner distance and the full width at half-maximum FWHM of the diffraction beaks were calculated as shown in Table 1, we can observe that the values of d and 2θ are nearly similar to that in the ASTM cards. The average crystallite size of thin film was determined using the Scherer's equation (Patterson,1939):

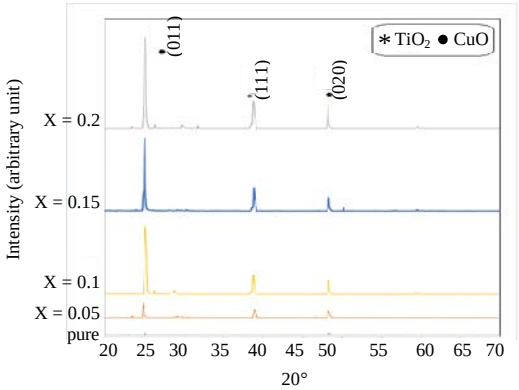

Fig. 2: The X-ray diffraction patterns for $(TiO_2)_{1-x}$, $(CuO)_x$ thin films at RT

Table 1: The peaks and its Bragg's angles, interplanar distance and full width at half-maximum for $(TiO_2)_{1-x}$, (CuO) xthin films at different concentrations of CuO

Content	2θ°	FWHM°	Int (Arab. unit)	Dhkl Exp. (Å)	G.S (nm)	D_{hkl} Std.	Phase	Hkl	Card No.
Pure	25.10	0.2083	28	3.5444	39.1	3.5169	TiO_2	011	96-900-9087
	48.44	0.2083	28	1.8778	41.8	1.8925	TiO_2	020	96-900-9087
x = 0.05	24.90	0.2083	167	3.5736	39.1	3.5169	TiO_2	011	96-900-9087
	38.96	0.4167	105	2.3100	20.2	2.3158	CuO	111	96-410-5686
	48.33	0.4167	77	1.8816	20.9	1.8925	TiO_2	020	96-900-9087
x = 0.1	25.10	0.3125	823	3.5444	26.0	3.5169	TiO_2	011	96-900-9087
	38.75	0.4167	237	2.3219	20.2	2.3158	CuO	111	96-410-5686
	48.33	0.2083	181	1.8816	41.8	1.8925	TiO_2	020	96-900-9087
x = 0.15	25.10	0.3125	872	3.5444	26.0	3.5169	TiO_2	011	96-900-9087
	38.85	0.4167	300	2.3159	20.2	2.3158	CuO	111	96-410-5686
	48.33	0.3225	174	1.8816	27.9	1.8925	TiO_2	020	96-900-9087
x = 0.2	25.10	0.3125	1088	3.5444	26.0	3.5169	TiO_2	011	96-900-9087
	38.85	0.4167	328	2.3159	20.2	2.3158	CuO	111	96-410-5686
	48.23	0.2083	272	1.8854	41.8	1.8925	TiO_2	020	96-900-9087

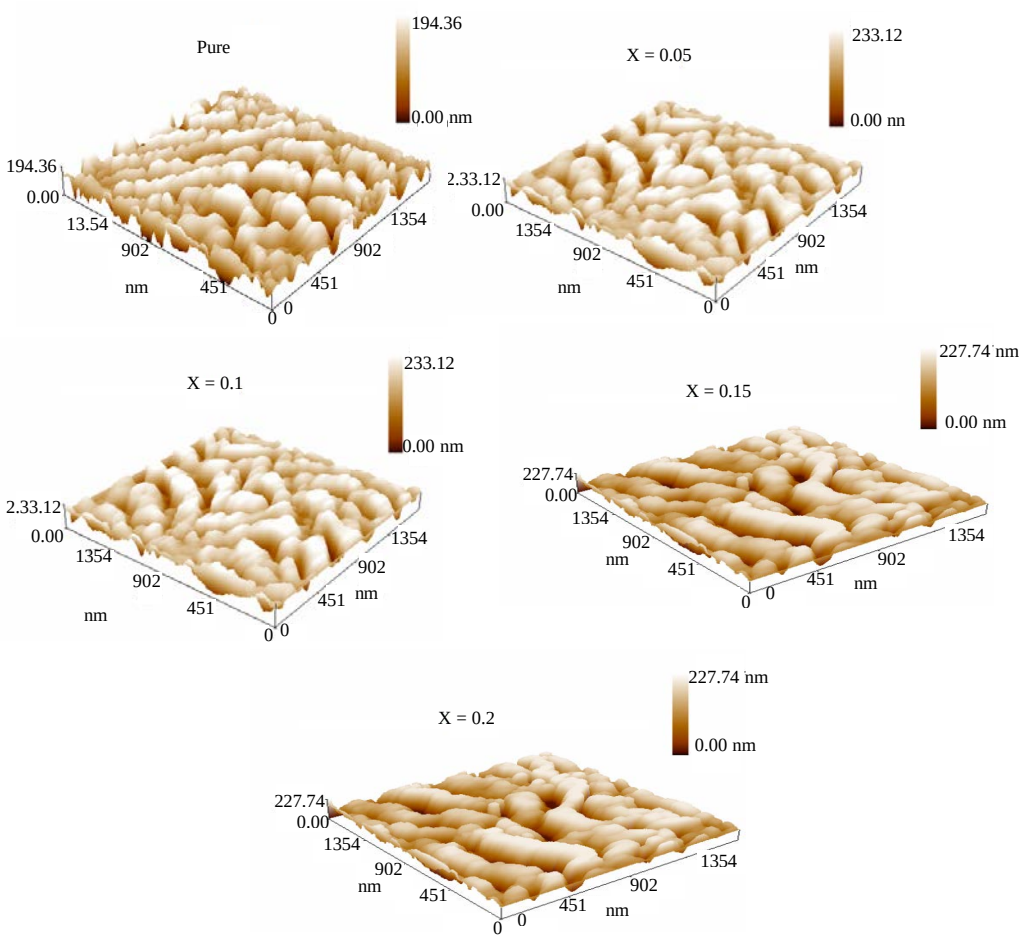

Fig. 3: AFM images for $(TiO_2)_{1-x}(CuO)_x$ thin films at different concentrations of CuO

$$G = 0.94\,\lambda/\beta\,\cos\theta \quad (1)$$

Where:

G = The average crystalline size

λ = The X-ray wavelength

β = The Full-Width at Half Maximum (FWHM) in radian

θ = The Bragg diffraction angle in degree

It is cleared from the Table 1, that d_{hkl} and grain size increases with increasing of value of x. This implies that Cu partially substituted for Ti in TiO_2 structure.

AFM studies: Surface morphologies obtained through Atomic Force Microscope (AFM) of pure and CuO-doped TiO_2 films are shown in Fig. 3. We find considerable

Table 2: Average roughness, grain size and RMS roughness for the $(TiO_2)_{1-x}$, $(CuO)_x$ thin films at different concentrations of CuO obtained from (AFM)

Contents	Average grain	Average roughness (nm)	RMS (nm)
Pure	51.40	42.10	49.9
0.05	52.35	50.80	59.5
0.1	89.00	51.10	60.8
0.15	87.09	52.00	61.0
0.2	106.00	52.99	69.0

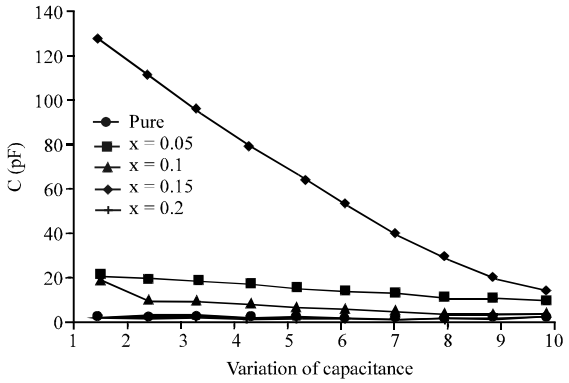

Fig. 4: The variation of capacitance versus reverse bias voltage for $(TiO_2)_{1-x}(CuO)_x$/p-Si heterojunctions at a frequency of 0.5 kHz for different concentrations of CuO

roughness of films surface. It is observed that the films surface roughness increases with concentration. This might be attributed to the increases of the average grain size with increasing concentration. Also, it is observed that the average grain size increases with increasing of concentration. Table 2 average roughness, grain size and RMS for the $(TiO_2)_{1-x}$, $(CuO)_x$ thin films at different concentrations of CuO obtained from (AFM).

According to AFM images in Fig. 2, TiO_2 morphology is completely changed after doping with 2% CuO and increases the efficiency.

C-V characteristic: The capacitance versus reverse voltage (C-V) measurements were used to determine (V_{bi}) (the built in potential). The barrier height and the width of depletion layer (W). The variation of capacitance as a function of reverse bias voltage in the range (0-1) for $(TiO_2)_{1-x}$, $(CuO)_x$/p-Si heterojunctions as shown in Fig. 4 and 5, respectively. This measurements were achieved in frequencies 0.5 and 1 kHz. It is obvious that the measured capacitance is decreased with increasing of the reverse bias voltage this behavior is attributed to the increase of the depletion region width which leads to the increase of the built-in voltage. It can be observed from Table 3, that the capacitance at zero bias voltage (Co) decreases with increasing CuO content for all the prepared junctions. This is attributed to the decrease in the surface states which leads to an increase in the depletion layer width and a decrease of the capacitance. Also, this result is

Table 3: Values of zero capacitance and bias voltage for $(TiO_2)_{1-x}(CuO)_x$/p-Si heterojunctions at different frequencies and different concentrations of CuO

Frequency (kHz)	Content	C_o (pF)	V_{bi} (Volt)
	Pure	140	0.12
	0.05	30	0.15
0.5	0.10	22	0.21
	0.15	4	0.30
	0.20	0.998	0.40
	Pure	40	0.20
	0.05	11.65	0.40
1	0.10	8.89	0.50
	0.15	5	0.60
	0.20	4.86	0.70

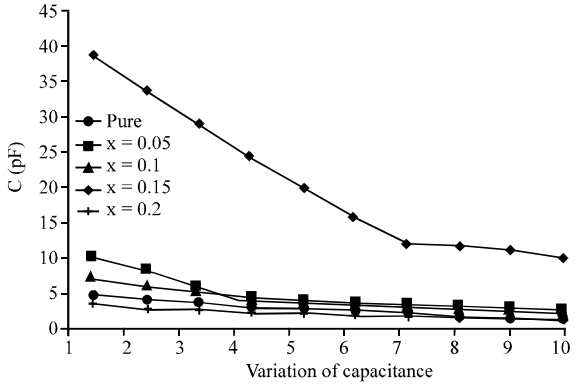

Fig. 5: The variation of capacitance versus reverse bias voltage for $(TiO_2)_{1-x}$, $(CuO)_x$/p-Si heterojunctions at a frequency of 1 KHz for different concentrations of CuO

confirmed by the equation: ($C = A'\epsilon s/t$) where A' is the active area of the junction and ϵs is the dielectric constant of the semiconductor layer.

Figure 6 and 7 show the inverse of the capacitance squared plotted against the applied reverse bias voltage for (TiO2)1-x(CuO) x/p-Si heterojunctions at different frequencies and different CuO concentration. The plots show a straight line relationship which means that the junction is of an abrupt type. The interception of the straight line with the voltage axis at (1/C2 = 0), represents the built in Voltage (Vbi). In general, it can be observed, from Table 3, that the built in voltage increases with increasing the CuO content as a result of the decrease in the capacitance value.

I-V characteristics: The I-V characteristic curves under dark and illumination of incident photon of the $(TiO_2)_{1-x}$, $(CuO)_x$/Si devices at different concentration of CuO are shown in Fig. 8. A summary of the efficiency and Parameters estimated from the I-V curves under illumination is presented in Table 3. The solar conversion efficiency was calculated using the following equation (Chan *et al*., 1986):

$$\eta = \frac{V_{oc} \times I_{sc}}{P_{in}} FF \quad (2)$$

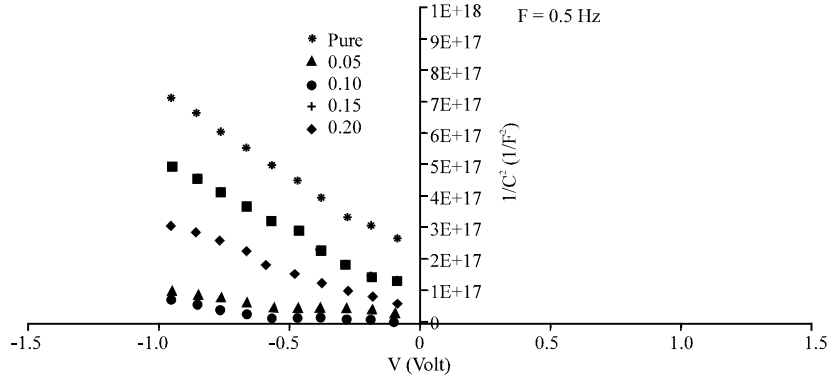

Fig. 6: The inverse of capacitance squared against applied reverse bias voltage for $(TiO_2)_{1-x}$, $(CuO)_x$/p-Si heterojunctions at frequency 0.5 kHz and different concentrations of CuO

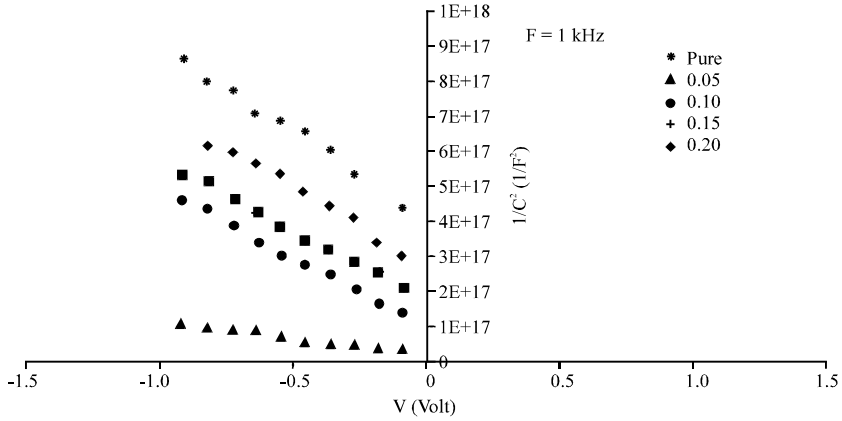

Fig. 7: The inverse of capacitance squared against applied reverse bias voltage for $(TiO_2)_{1-x}(CuO)_x$/p-Si heterojunctions at frequency 1 kHz and different concentrations of CuO

Table 4: Efficiency and parameters

Content	I_{sc} (mA)	V_{oc} (V)	I_m (mA)	V_m (v)	FF	η	β
Pure	1.000	0.900	0.750	0.600	0.500	1.125	2.657
0.05	1.100	1.100	0.850	0.550	0.386	1.169	2.335
0.1	1.000	1.050	0.800	0.700	0.533	1.400	2.213
0.15	1.000	1.050	0.800	0.700	0.533	1.400	2.336
0.2	1.000	1.600	0.900	0.950	0.534	2.138	2.999

Where:
V_{oc} = Open circuit Voltage (V)
I_{sc} = Short circuit current (mA/cm^2)
FF = Fill factor (Chan *et al*., 1986)

$$FF = \frac{V_m \times I_m}{V_{oc} \times I_{sc}} \quad (3)$$

where, V_{max} and I_{max} are voltage and current at the point of maximum power output of the cell. It was observed the short circuit currents (I_{sc}), show slight variation while the open circuit Voltages (V_{oc}) and Fill Factors (FF) values show long variation. Also, it can be cleared that the addition of CuO to the TiO_2 films show an increase in the efficiency of the solar cell. It is observed from Table 3 that the efficiently for the doped film is around one times more than that of undoped TiO_2 films.

The [I_{sc}], [V_{oc}], [FF] and conversion efficiency of the fabricated solar cell were 1.0 mA, 1.6 V, 0.534 and 2.138%, respectively. According to our knowledge, the reported values of I_{sc}, V_{oc}, FF and efficiency in this research represent the highest reported values as compared to previous work for this material. Results show that TiO_2:CuO nanocomposite is a good selection and improves the solar cell efficiency.

Table 4 shows the efficiency and Parameters estimated from the I-V curves under for $(TiO_2)_{1-x}$, $(CuO)_x$/Si solar cell at different concentrations of CuO.

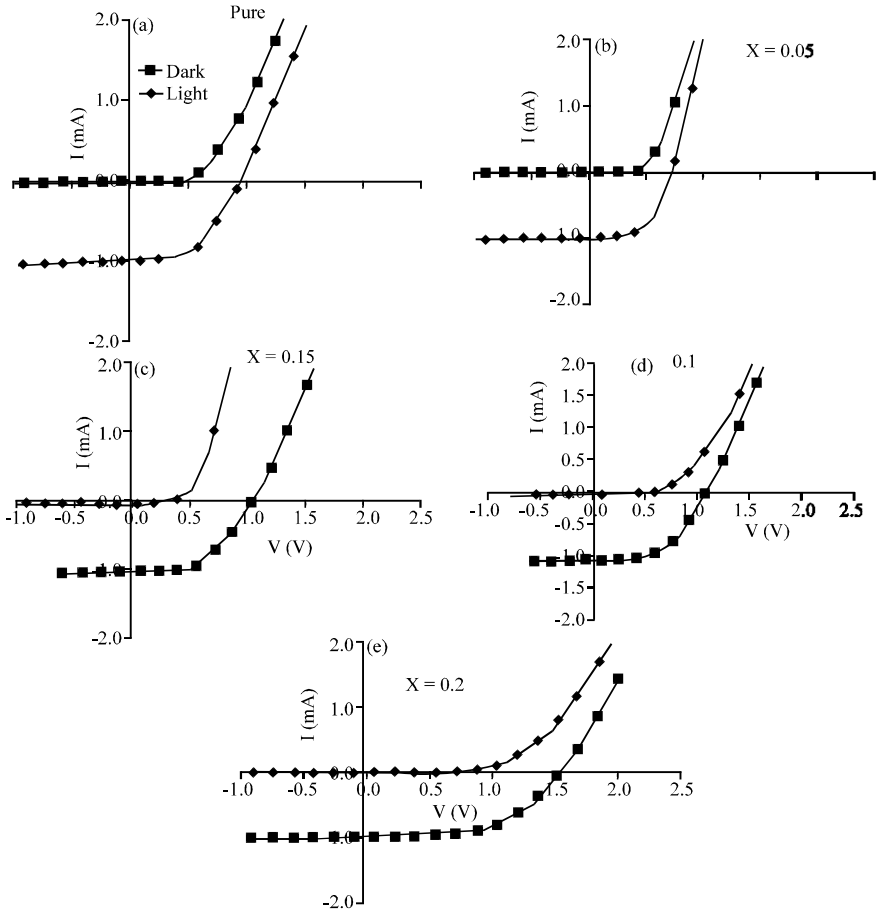

Fig. 8: Dark and light I-V characteristics of $(TiO_2)_{1-x}$, $(CuO)_x$/Si devices at different concentrations of CuO

CONCLUSION

In this research, we have deposited and characterized Laser Induced Plasma technique was used to prepare undoped and CuO-doped TiO_2 solar cell on Si substrate. that performs a short-circuit photocurrent density (I_{sc}) of 1mA , an open-circuit Voltage (V_{oc}) of 1600 mV and a Fill Factor (FF) of 0.534, corresponding to an overall conversion efficiency of 0.2138%. XRD and AFM measurements were carried out for the films at room temperature. However, its efficiency can be increased with the addition of CuO and can further be improved by the structure was found. The above result may be utilized to design an efficient efficiency of solar cell.

REFERENCES

Banerjee, A.N. and K.K. Chattopadhyay, 2005. Recent developments in the emerging field of crystalline P-type transparent conducting oxide thin films. Prog. Crystal Growth Charact. Mater., 50: 52-105.

Chan, D.S.H., J.R. Phillips and J.C.H. Phang, 1986. A comparative study of extraction methods for solar cell model parameters. Solid State Electron., 29: 329-337.

Dijkkamp, D., T. Venkatesan, X.D. Wu, S.A. Shaheen and N. Jisrawi *et al.*, 1987. Preparation of Y-Ba-Cu oxide superconductor thin films using pulsed laser evaporation from high TC bulk material. Appl. Phys. Lett., 51: 619-621.

Gartner, M., C. Parlog and P. Osiceanu, 1993. Spectroellipsometric characterization of lanthanide-doped TiO_2 films obtained via the sol-gel technique. Thin Solid Films, 234: 561-565.

Kozlowski, M.R., P.S. Tyler, W.H. Smyrl and R.T. Atanasoski, 1989. Anodic TiO_2 thin films photoelectrochemical, electrochemical and structural study of heat-treated and modified films. J. Electrochem. Soc., 136: 442-450.

Leprince-Wang, Y. and K. Yu-Zhang, 2001. Study of the growth morphology of TiO_2 thin films by AFM and TEM. Surf. Coat. Technol., 140: 155-160.

Linsebigler, A.L., G. Lu and J.T. Yates Jr, 1995. Photocatalysis on TiO_2 surfaces: Principles, mechanisms and selected results. Chem. Rev., 95: 735-758.

Lottiaux, M., C. Boulesteix, G. Nihoul, F. Varnier and F. Flory *et al*., 1989. Morphology and structure of TiO_2 thin layers vs thickness and substrate temperature. Thin Solid Films, 170: 107-126.

Mazhir, S.N. and N.H. Harb, 2015. Influence of concentration on the structural, optical and electrical properties of TiO_2: CuO thin film fabricate by PLD. IOSR. J. Appl. Phys., 7: 14-21.

Mazhir, S.N., 2018. Spectroscopic study of (TiO2)1-x(CuO)x Plasma generated by Nd: YAG laser. ARPN. J. Eng. Appl. Sci., 13: 864-869.

Mazhir, S.N., G.H. Mohamed, A.A. Abdullah and M.D. Radhi, 2015. UV photovoltaic detector based on Bi doped TiO2 fabricated by pulse laser deposition. Int. J. Adv. Res., 3: 1060-1070.

Mechiakh, R. and R. Bensaha, 2006. Analysis of optical and structural properties of Sol-Gel TiO_2 thin films. Moroccan J. Condens. Matter, 7: 54-57.

Meng, L.J., M. Andritschky and D.M.P. Santos, 1993. The effect of substrate temperature on the properties of DC reactive magnetron sputtered titanium oxide films. Thin Solid Films, 223: 242-247.

Messick, L., 1976. A GaAs/Si x O y N z MIS FET. J. Appl. Phys., 47: 5474-5475.

Oehrlein, G.S., 1986. Oxidation temperature dependence of the dc electrical conduction characteristics and dielectric strength of thin Ta2O5 films on silicon. J. Appl. Phys., 59: 1587-1595.

Oral, A.Y., E. Mensur, M.H. Aslan and E. Basaran, 2004. The preparation of copper (II) oxide thin films and the study of their microstructures and optical properties. Mater. Chem. Phys., 83: 140-144.

Papadimitropoulos, G., N. Vourdas, V.E. Vamvakas and D. Davazoglou, 2006. Optical and structural properties of copper oxide thin films grown by oxidation of metal layers. Thin Solid Films, 515: 2428-2432.

Patterson, A.L., 1939. The Scherrer formula for X-ray particle size determination. Phys. Rev., 56: 978-982.

Ristov, M., G.J. Sinadinovski and I. Grozdanov, 1985. Chemical deposition of Cu2O2 thin films. Thin Solid Films, 123: 63-67.

Smith, H.M. and A.F. Turner, 1965. Vacuum deposited thin films using a ruby laser. Appl. Opt., 4: 147-148.

Suhail, M.H., G.M. Rao and S.D.C.J. Mohan, 1992. DC reactive magnetron sputtering of titanium-structural and optical characterization of TiO_2 films. J. Appl. Phys., 71: 1421-1427.

Williams, L.M. and D.W. Hess, 1983. Structural properties of titanium dioxide films deposited in an RF glow discharge. J. Vac. Sci. Technol. A Vac. Surf. Films, 1: 1810-1819.

Wilmsen, C.N., 1985. Physics and Chemistry of Compound III-V Semiconductor Interfaces. Plenum Press, New York, USA., ISBN:9780306417696, Pages: 465.

Yaseen, H.M., B.G. Rasheed and S.N. Mazhir, 2016. Judd-ofelt analysis of spectroscopic properties of Er: TiO_2 prepared via sol-gel. IOSR. J. Res. Method Educ., 6: 30-33.

Yeung, K.S. and Y.W. Lam, 1983. A simple chemical vapour deposition method for depositing thin TiO_2 films. Thin Solid Films, 109: 169-178.

Yoon, K.H., W.J. Choi and D.H. Kang, 2000. Photoelectrochemical properties of copper oxide thin films coated on an n-Si substrate. Thin Solid Films, 372: 250-256.